Lafia Journal of Scientific & Industrial Research (LJSIR), Vol. 4(1), 2026
p-ISSN: 3026 – 9288 e-ISSN: 3027 – 1800 pages: 168-174
https://lafiascijournals.org.ng/index.php/ljsir/index ⇒ Published by the Faculty of Science,
Federal University of Lafia, Nasarawa State, Nigeria

Thermal Stability Analysis of Cassava Starch-Polyvinylpyrrolidone Nanocomposite Polymer Electrolytes using Kissinger Model for Lithium-ion Battery Applications

C. O. Iyamu*, I. I. Ewa & L. W. Lumbi
Department of Physics, Nasarawa State University, Keffi, Nigeria

Abstract

Due to the challenges faced by most electrolytes in withstanding high temperatures especially during peak operating conditions, this study analyses the thermal stability of cassava starch-polyvinylpyrrolidone nanocomposite polymer electrolytes for lithium-ion battery applications. The study employed five samples of cassava starch-polyvinylpyrrolidone nanocomposite polymer electrolytes prepared using direct-heating solution casting method. The data collected from these samples were analyzed using Bragg's, Sherrer's and Kissinger models. The results showed that all the samples are within the medium crystallite size and moderate activation energy range, with Sample 5 having the highest peak decomposition temperature and thermal stability of 194 KJ/mol.

Keywords: Nanocomposite polymer electrolyte, Cassava starch, Polyvinylpyrrolidone, Thermal stability, Activation energy, Kissinger model

Article History

Submitted
January 07, 2026

Revised
April 11, 2026

First Published Online
April 16, 2026

Correspondences
C. O. Iyamu ✉
caesariyamu71@gmail.com

doi.org/10.62050/ljsir2026.v4n1.776

Introduction

The increasing demand for safe, efficient, and high-performance energy storage systems has intensified research into solid-state polymer electrolytes as alternatives to conventional liquid electrolytes used in lithium-ion batteries (LIBs). Polymer electrolytes offer advantages such as flexibility, lightweight structure, good electrode-electrolyte contact, and improved safety by eliminating leakage and flammability concerns [1]. Despite these benefits, their practical application limited by challenges, including insufficient thermal stability, which can compromise battery performance and safety under elevated operating temperatures.

Thermal stability is a critical requirement for polymer electrolytes intended for lithium-ion battery applications, as batteries are frequently exposed to elevated temperatures during charging-discharging cycles and possible thermal runaway events. Poor thermal resistance can lead to polymer decomposition, electrolyte degradation, and device failure [2]. The thermal stability of nanocomposite polymer electrolytes is defined by the polymer segmental chain motion and nanofiller interfacial motion of nanoparticles [3]. As a result, polymers and nanoparticles play the greatest role in determining the rate of thermal degradation because their degradation suggests the thermal resistance ability of the electrolytes.

The Kissinger model [4], which is used to compute activation energy, is the theoretical model used to analyze thermal stability. TGA is widely used to investigate the thermal decomposition behavior of polymer electrolytes, providing information on degradation stages, mass loss profiles, and thermal endurance [5]. It measures the changes in sample mass as a function of temperature under controlled heating conditions, providing insights into moisture loss, decomposition stages, and thermal degradation profiles [6, 7].

The nanocomposite polymer electrolytes used in this study contain polymer materials, lithium salts, and additives, notably nanoparticles. These materials play a vital role in LIB performance. Although polymer materials play a significant role in thermal resistance, synthetic polymers, which are the most commonly used polymer electrolytes, contribute significantly to environmental challenges due to their toxic and non-biodegradable nature. In addition, their production and processing are expensive because of the high energy requirements and costs of raw materials. Altogether, these factors render them less sustainable than their biodegradable alternatives [8]. Raihan *et al.* [9] further emphasized that biodegradable materials are inexpensive, abundant, less toxic, and eco-friendly.

Biopolymer materials, such as cellulose and starch derivatives, have recently emerged as alternatives to synthetic polymers in energy storage systems because of their polymer chain flexibility. However, they require further optimization for high-performance applications [10]. Studies on cassava starch (CS) biopolymers, which are used either wholly or partially

to replace synthetic polymers in nanocomposite polymer electrolytes, are relatively new compared with numerous studies on polymer electrolytes that utilize only synthetic polymers [11]. Biopolymer-based polymer electrolytes have attracted increasing attention owing to their renewability, biodegradability, low cost, and environmental sustainability. A starch-based biopolymer is a naturally abundant polysaccharide with a high density of hydroxyl functional groups that facilitate salt dissociation and ion transport [12]. However, starch-based electrolytes generally suffer from low thermal resistance and structural instability caused by strong intermolecular hydrogen bonding and partial crystallinity, which restrict their high-temperature performance [13].

The need to investigate the composite blend of CS and polyvinylpyrrolidone (PVP) in nanocomposite polymer electrolytes arises from the goal of developing more sustainable, thermal resistance, and efficient materials for energy storage applications. This study analyzed the thermal stability of cassava starch-polyvinylpyrrolidone nanocomposite polymer electrolytes using a Kissinger model for LIB application.

Theoretical Models

Bragg's law and the Scherrer model

Bragg's law and the Scherrer model [14] form the basis of X-ray Diffraction (XRD), which scans the bulk crystalline structure of materials to reveal crystalline phase patterns.

Bragg's law is defined as:

$$n\lambda = 2dsine\,\theta \qquad (1)$$

Where, n= order of diffraction of the sample (an integer 1, 2, 3…); λ=X-ray wavelength of the sample; d= distance between the neighboring atomic layers (d-spacing) of the sample; θ= reflection angle the sample

Scherrer's model is:

$$D = \frac{K\lambda}{\beta \cos\theta}$$

Where: D = crystallite size (nm) of the sample; K= shape factor (0.9) for polymer electrolytes; λ= X-ray wavelength computed from Bragg's law; β = full width at half maximum (FWHM) in radians; θ = Bragg angle (in radians)

The Kissinger model

The Kissinger model is used to determine the activation energy (E_a) of a material's decomposition using TGA data [4]. The Kissinger equation is as follows:

Kissinger equation: $\ln\left(\frac{\beta}{T_P^2}\right) = \ln\left(\frac{AR}{E_a}\right) - \frac{E_a}{R\,T_p}$ (2)

The rearranged Kissinger equation becomes,

$$\frac{E_a}{R\,T_p} = \ln\left(\frac{AR}{E_a}\right) - \ln\left(\frac{\beta}{T_P^2}\right) \qquad (3)$$

Where: β= heating rate (K/min or ^{o}C/min); T_p= peak temperature (in kelvin); E_a = activation energy (K J/mol); A = pre-exponential factor (S^{-1}) for polymer degradation, which is generally within the range of 10^{10} to 10^{13} s^{-1} [5]; R = gas constant (8.314 J/mol. K)

Vijaya *et al.* [15] gave the following criterion for thermal stability:

i. Low thermal stability (low activation energy): <100 KJ/mol
ii. Moderate thermal stability (activation energy): 100-200 KJ/mol
iii. High thermal stability (high activation energy): >200 kJ/mol

Materials and Methods

Materials

The materials used in this work consist of lithium acetate dihydrate $(LiOOCCH_3.2H_2O)$ (99 %), PVP (98 %), CS powder (95 %), titanium dioxide (TiO_2(99 %), borax (98 %), glycerol (98 %), and deionized water (99.9 %). CS powder was locally prepared, while $LiOOCCH_3.2H_2O$, PVP, TiO_2, borax, glycerol and deionized water were purchased through a vendor at African University of Science and Technology, Galadima, FCT-Abuja.

Preparation of cassava starch powder

CS powder wasprepared based on [15] procedures. The procedures involved washing and peeling off the skin of a cassava tubers. The peeled tubers were then disintegrated by grinding using industrial grinding processor. The grinded tubers were then placed in deionized water, stirred for 15 min, and filtered through muslin cloth. The filtered liquid was left to settle down for 12 h, to allow it to precipitate. The precipitated starch was obtained after removing water left on top of it. The precipitated CS was then washed three times with deionized water and dried in an oven for 24 h at $50\,^{0}C$. The dried precipitated CS was then grinded using household electric grinding machine to obtain CS powder.

Preparation of nanocomposite polymer electrolyte films

The nanocomposite polymer electrolyte films were prepared using direct heating solution casting method as illustrated by Slesarenko *et al.* [16]. The nanocomposite polymer electrolyte materials composition is presented on Table 1.

Table 1: Compositions of CS- PVP nanocomposite polymer electrolytes

Sample	CS (g)	PVP (g)	Glycerol (ml)	Borax (g)	Titanium Dioxide (g)	Lithium Acetate Dehydrate (g)
S1	0	5	2	0.3	0.15	0.5
S2	1.5	3.5	2	0.3	0.15	0.5
S3	2.5	2.5	2	0.3	0.15	0.5
S4	3.5	1.5	2	0.3	0.15	0.5
S5	5	0	2	0.3	0.15	0.5

Based on the above material compositions, five CS-PVP nanocomposite polymer electrolyte samples were prepared using the direct-heat solution casting method.

As shown in Fig. 1, CS and PVP solutions were prepared using 15-50 mL of deionized water. The solution was then heated at 60 ^0C for 30 min and stirred using a magnetic stirrer at 750 rpm. After 30 min, glycerol was added and mixed for another 10 min. Subsequently, borax and TiO_2 were added and further mixed for another additional 10 min. Finally, lithium acetate dihydrate was added and mixed with the solution for another 20 min. At end of the 20 min, the solution was cast onto three Teflon sheets and dry at room temperature for 48 h. The dried films were then peeled off using a razor blade and used for the experiments.

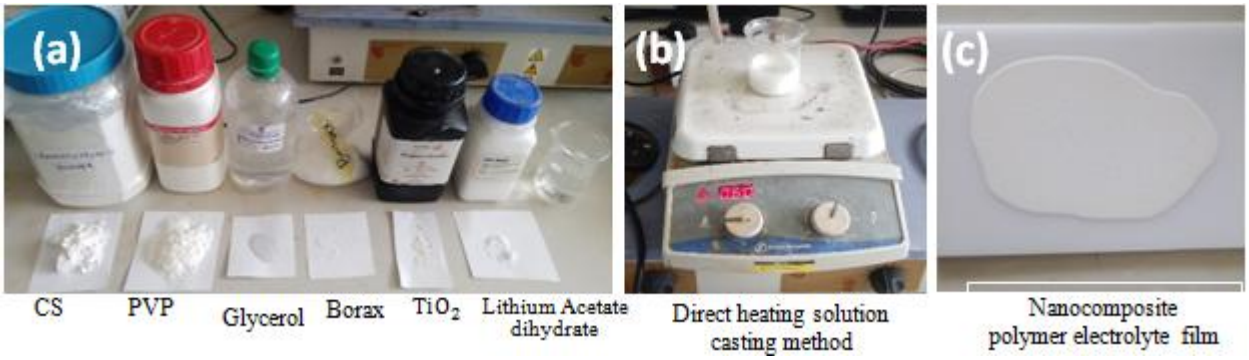

Figure 1: (a) Materials of CS-PVP nanocomposite polymer electrolytes, (b) The prepared polymer electrolyte solutions, based on the sample compositions, were heated on a hot-plate magnetic stirrer. In addition, a magnetic stirrer bar was placed inside the solution to ensure uniform mixing, (c) Nanocomposite polymer electrolytes placed on a Teflon sheet, and allow to dry at room

X-ray diffraction

XRD was used to collect data on the internal structure of nanocomposite polymer electrolyte films. PANanalytical X'Pert PRO diffractometer was used to scan the internal structure of the sample, and it was performed over a (2θ) of 5° to 80° with a step size of 0.02° and a scan speed of $1°/min$.XRD data were analyzed using Bragg's law and Scherrer's model to derive the crystallite size [14].

Thermogravimetric analysis

TGA (PerkinElmer TGA 4000) was used to record thermal stability data from 30 to 950 ^0C at a heating rate of $10\,^0C/min$, producing weight-loss versus temperature plots. Kissinger model was then applied to TGA data to compute the activation energy of thermal degradation, which is used to quantify thermal stability [4, 13].

Results and Discussion

X-ray diffraction

The XRD plots of the samples are presented in Figs 2–6. The crystallite sizes of the nanocomposite polymer electrolytes analyzed using Bragg's law and Scherrer's model are presented in Table 2–6.

The XRD patterns of samples 1-5 (Fig. 2-6), revealed the presence of multiple crystalline phases, including urea, graphite, tridymite, and silicalite, including a heterogenous structural organization within the nanocomposite polymer electrolytes. Notably, the sharpest diffraction peaks appear between $15° - 30°2\,\theta$, suggesting well-ordered crystalline domains that provide structural stability while maintaining sufficient polymer chain flexibility.

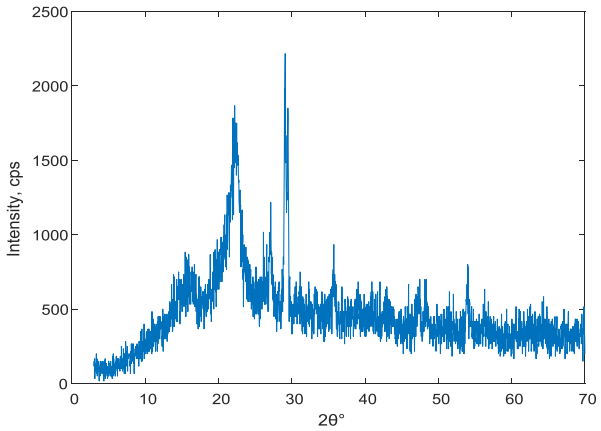

Figure 2: XRD plot of sample 1 (0 g CS: 1.5 g PVP) performed at a scan speed of $1°/min$

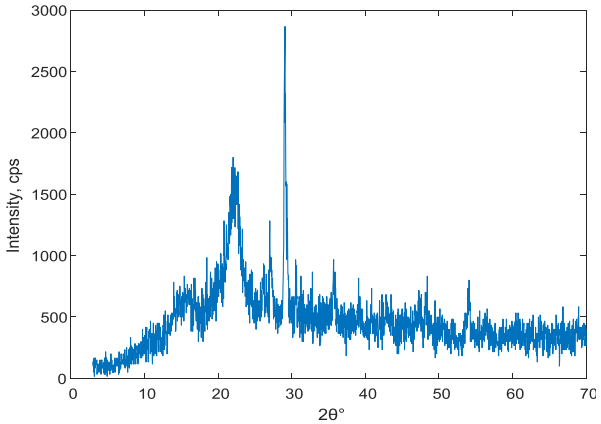

Figure 3: XRD plot of sample 2 (1.5 g CS: 3.5 g PVP) performed at a scan speed of$1°/min$

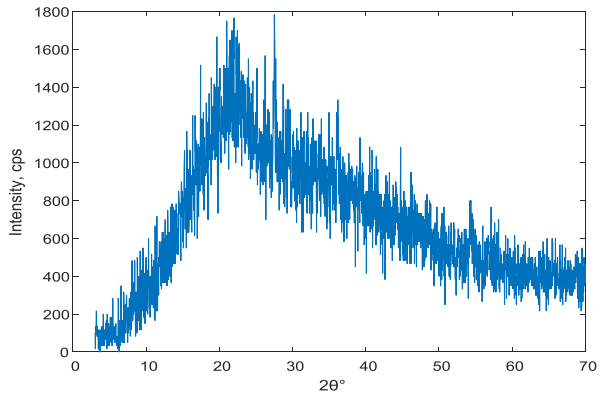

Figure 4: XRD plot of sample 3 (2.5 g CS: 2.5 g PVP) performed at a scan speed of$1°/min$

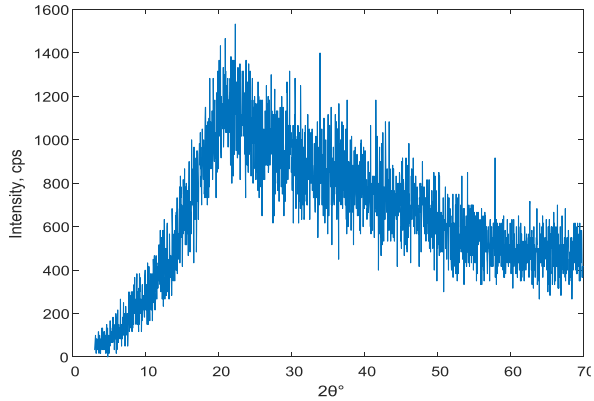

Figure 5: XRD plot of sample 4 (3.5 g CS: 1.5 g PVP) performed at a scan speed of $1°/min$

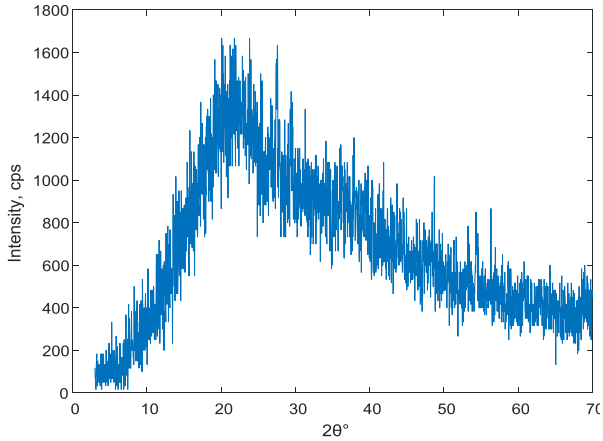

Figure 6: XRD plot of sample 5 (5 g CS: 0 g PVP) performed at a scan speed of$1°/min$

Table 2: Crystallite size result of sample 1 (0 g CS: 1.5 g PVP) at order of diffractions 1-4

N/S	θ Rad.	FWHM (β) Rad.	λ, Å	K	d, Å	D, nm
1	0.196	0.028	1.542	0.9	3.959	5.05
2	0.236	7.68 x10^{-3}	0.769	0.9	3.290	9.27
3	0.254	9.599 x10^{-3}	0.514	0.9	3.0689	4.98
4	0.294	5.59 x10^{-3}	0.365	0.9	2.516	6.14
				Average D		**6.36 nm**

Table 3: Crystallite size result of sample 2 (1.5 g CS: 3.5 g PVP) at order of diffraction 1-7

N/S	θ Rad.	FWHM (β) Rad.	λ, Å	K	d, Å	D, nm
1	0.126	0.0297	1.5406	0.9	6.13	4.71
2	0.139	0.021	0.770	0.9	5.56	3.33
3	0.194	0.035	1.538	0.9	3.989	4.03
4	0.237	8.90 x10^{-3}	0.385	0.9	3.283	4.01
5	0.254	4.01 x10^{-3}	0.309	0.9	3.0698	7.17
6	0.294	5.93 x10^{-3}	0.240	0.9	2.5158	3.80
7	0.472	8.20 x10^{-3}	0.22	0.9	1.6931	2.71
				Average D		**4.25 nm**

Table 4: Crystallite size result of sample 3 (2.5 g CS: 2.5 g PVP) at order of diffraction 1

N/S	θ Rad.	FWHM (β) Rad.	λ, Å	K	d, Å	D, nm
1	0.193	0.4503	1.541	0.9	4.018	**31.4 nm**

Table 5: Crystallite size result of sample 4 (3.5 g CS: 1.5 g PVP) at order of diffraction 1

N/S	θ Rad.	FWHM (β) Rad.	λ, Å	K	d, Å	D, nm
1	0.214	0.548	1.54	0.9	3.63	**25.9 nm**

Table 6: Crystallite size result of sample 5 (5 g CS: 0 g PVP) at order of diffraction 1

N/S	θ Rad.	FWHM (β) Rad.	λ, Å	K	d, Å	D, nm
1	0.192	0.433	1.538	0.9	4.03	**32.6 nm**

Sample 5 exhibited the largest crystallite size of 32.6 nm, which, combined with its sharp peaks, reflects medium crystallinity. This intermediate degree of order is significant: It ensures mechanical reinforcement from the crystalline regions while retaining amorphous segments that facilitate ion mobility. Such a balance is critical for solid-state electrolytes, as excessive crystallinity can hinder lithium-ion transport, whereas insufficient order may compromise structural integrity.
The multiphase composition likely contributes synergistically to electrolyte performance: silicate and tridymite enhance thermal and mechanical stability, graphite provides conductive pathways, and urea influences polymer chain packing. The observed diffraction features align with previous studies of many researchers [17, 9, 18], which demonstrated that medium crystallinity optimizes both mechanical and ionic properties in polymer electrolytes.

Thermal stability and activation energy

The activation energies of Samples 1-5 were analyzed using Kissinger model as presented in Figs 7–11 and Table 7.

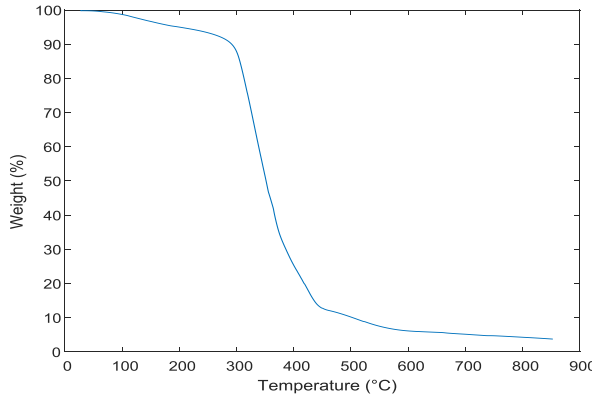

Figure 7: TGA plot of sample 1 (0 g CS: 5 g PVP) recorded from 30 to 950 ^0C heating temperature, and at a heating rate of 10 $^0C/min$

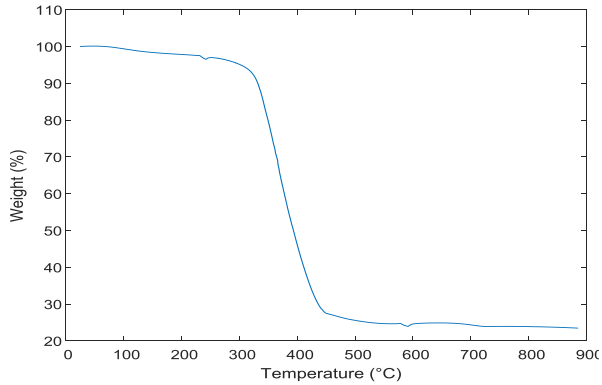

Figure 8: TGA plot of sample 2 (1.5 g CS: 3.5 g PVP) recorded from 30 to 950 ^0C heating temperature, and at a heating rate of 10 $^0C/min$

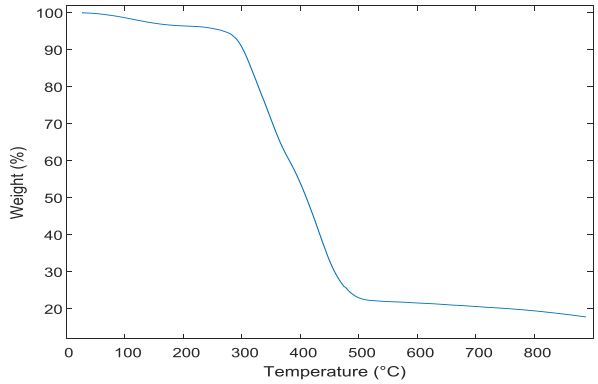

Figure 9: TGA plot of sample 3 (2.5 g CS: 2.5 g PVP) recorded from 30 to 950 ^0C heating temperature, and at a heating rate of 10 $^0C/min$

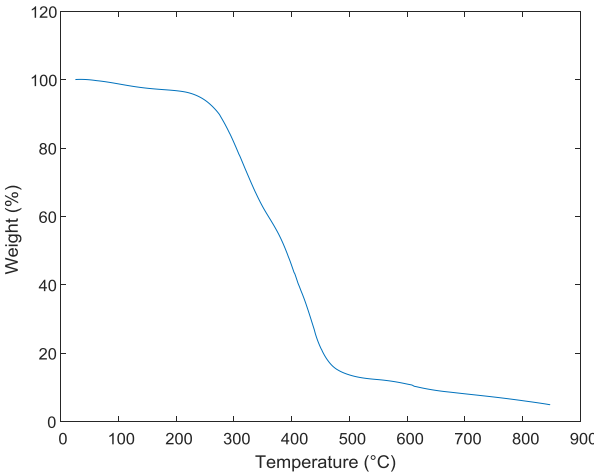

Figure 10: TGA plot of sample 4 (3.5 g CS: 1.5 g PVP) recorded from 30 to 950 ^0C heating temperature, and at a heating rate of 10 $^0C/min$

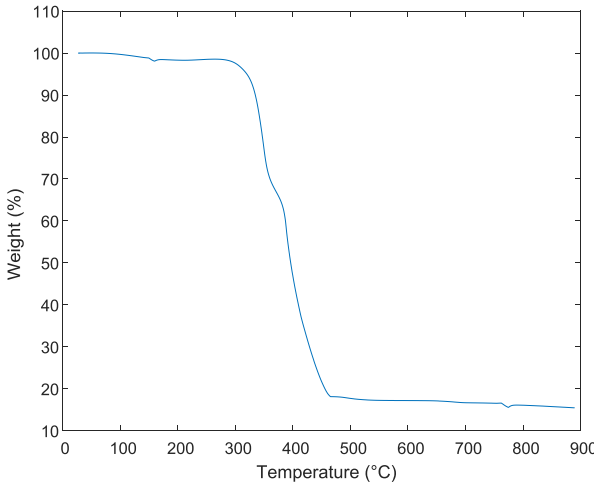

Figure 11: TGA plot of sample 5 (5 g CS: 0 g PVP) recorded from 30 to 950 ^0C heating temperature, and at a heating rate of 10 $^0C/min$

Table 7: Activation energies of samples 1-5 computed at a heating rate of 10 $^0C/min$

Sample	Heating Rate, β (K/s)	Peak temperature of Samples, Tp (K)	Pre-Exponential Factor, A (s^{-1})	Gas constant, R (KJ/mol K)	Activation energy (Ea) (KJ/mol)
1(0 g CS: 5 g PVP)	0.1667	623.15	10^{13}	$8.314x10^{-3}$	179
2(1.5g CS: 3.5g PVP)	0.1667	643.15	10^{13}	$8.314x10^{-3}$	185
3(2.5 g CS: 2.5 g PVP)	0.1667	653.15	10^{13}	$8.314x10^{-3}$	188
4(3.5 g CS: 1.5 g PVP)	0.1667	658.15	10^{13}	$8.314x10^{-3}$	189
5(5 g CS: 0 g PVP)	0.1667	673.15	10^{13}	$8.314x10^{-3}$	194

Sample 5 exhibited the highest activation energy of 194 kJ/mol, while the other samples fell within the range of 100-200 KJ/mol, indicating moderate thermal stability as reported in the literature [13]. The higher activation energy of sample 5 suggests stronger intermolecular interactions and a more stable polymer structure, requiring greater energy for thermal degradation.

This behavior can be linked to its structural characteristics, particularly its medium crystallinity and multiphase composition. The presence of crystalline regions restricts polymer chain mobility at elevated temperatures, thereby enhancing thermal resistance, while the amorphous regions maintain segmental flexibility necessary for ion transport.

The moderate thermal stability observed across all samples reflects a balance between structural rigidity and polymer mobility. This is important in polymer electrolytes, where sufficient thermal resistance must coexist the ability of polymer chains to support ionic conductivity. The present results are consistent with previous studies [19–22, 24], which reported stable polymer electrolytes above 100 ^{o}C. However, the findings differ from reports [15, 23] of lower stability, likely due to differences in composition, lower crystallinity, and the absence of reinforcing phases, which reduce resistance to thermal degradation.

Conclusion

The structural and thermal analyses provide important insights into the behavior of the developed nanocomposite polymer electrolytes. The XRD results confirmed the presence of multiple crystalline phases and moderate crystallinity across the samples, with sample 5 exhibiting the largest crystallite size and more defined crystalline features, indicating a more organized structure. The thermal analysis showed that all samples possess moderate thermal stability, with activation energies within the range of 100 – 200 kJ/mol. Notably, sample 5 exhibited the highest the highest activation energy (194 kJ/mol), indicating superior thermal stability compared to the other samples. This enhanced stability is attributed to its structural characteristics, particularly its balanced crystalline-amorphous nature and multiphase composition.

These findings demonstrate that variations in structural organization significantly influence thermal behavior, and that optimizing crystallinity and phase composition can enhance the performance of polymer electrolytes for solid-state lithium-ion battery applications.

Conflict of interest: The authors declare no conflicts of interest.

References

[1] Andersson, R., Hernandez, G., See, J., Flaim, T. D., Brandell, D. & Mindemark, J. (2022). Designing polyurethane solid polymer electrolytes for high temperature lithium metal batteries. *ACS Appl. Energy Material*, 1, 407-418. https://doi.org/10.1021/acsaem.1c02942

[2] Arrieta, A. A., Calabokis, O. P. & Mendoza, J. M. (2023). Effect of lithium salts on the properties of cassava starch on solid biopolymer electrolytes. *Polymers*, 15(20), 1-3. https://doi.10.3390/polym1520450

[3] Arrieta, A. A., Calabokis, O. P. & Vanegas, C. (2024). Influence of lithium triflate salt concentration on structural, thermal, electrochemical, and ionic conductivity properties of cassava state solid biopolymer electrolytes. *Int. J. of Molecular Sci.*, 25(15), 8450. https://doi.org/10.3390/ijms25158450

[4] Cullity, B. D. & Stock, S. R. (2014). *Elements of X-ray Diffraction* (3rd edition). Pearson Educational Limited. www.pearsoned.co.uk

[5] Gustav, E. (2016). A study of poly (vinyl alcohol) as a solid polymer electrolyte for lithium ion batteries. *Uppsala Universitet.* http://www.teknat.uu.se/student

[6] Hamsan, M. H., Nofal, M. M., Aziz, S. B., Biza, M. A., Dannoun, E. M. A., Murad, A. R., Kadir, M. F. D. & Muzakir, S. K. (2021). Plasticized polymer blend electrolyte based on chitosan for energy storage application: Structural, circuit modeling, morphological and electrochemical properties. *Polymers*, 13, 1233. https://doi.org/10.3390/polym13081233.

[7] Huang, X., Leng, X., Li, T., Wang, C., Tang, T., Xie, L., Liu, B. & Zhang, S. (2024). TiO_2 inorganic nanoparticle framework enhanced PEO based solid-state electrolytes for improved performance of solid-state lithium batteries. *ResearchSquare Platform LLC.* https://doi.org/10.21203/rs.3.rs-4136142/v1

[8] Ma, Q., Qi, X., Tong, B., Zheng, Y., Feng, W., Nie, J., Hu, Y., Li, H., Huang, X., Chen, L. & Zhou, Z. (2016). Novel Li (CF_3SO_2) (n-$C_4F_9SO_2$) N based polymer electrolytes for solid state lithium batteries with superior electrochemical performance. *ACS Applied Material and Interfaces*, 8(43), 29705-29712. https://doi.org/10.1021/acsami.6b10597

[9] Raihan, R., Fairuzdzah, A. L., Asiah, M. N. & AbMalik, M. A. (2022). The compatibility of jackfruit seed starch and polyvinyl alcohol blend as biopolymer electrolyte host. *Malaysian J. of Analyt. Sci.*, 26(4), 829-837. https://mjas.analis.com.my/mjas/v26_n4/pdf/Raihan_26_4_13.pdf

[10] Ruiqu, H.R., Kazuaki, M. & Masayuki, Y. (2025). Eco-friendly adhesion of isosorbide-based polycarbonate. *Molecules*, 30(13), 2843. https://doi.org/10.3390/molecules30132843

[11] Patra, N., Ramesh, P., Donthu, V. & Ahmad, A. (2024). Biopolymer-based composites for sustainable energy storage: Recent developments and future outlook. *Journal of Materials Sci.: Materials in Engr.*, 19(1), 34. https://doi.org/10.1186/s40712-024-00181-9

[12] Liew, C. W., Ramesh, S., Ramesh, K. & Arof, A. K. (2012). Preparation and characterization of lithium ion conducting ionic liquid-based biodegradable corn starch polymer electrolytes. *J. of Solid-State Electrochemistry*. https: //doi.org/10.1007/s10008-012-1651-5

[13] Raut, P., Li, S., Chen, Y., Zhu, Y. & Jana, S.C. (2019). Strong and flexible composite solid polymer electrolyte. Membranes for Li-ion batteries. *ACS Omega*, 4, 18203-18209. https://doi.org/10.1021/acsomega.9b00885

[14] Shahrudin, S. & Ahmad, A. H. (2016). Corn starch-based biopolymer electrolyte doped with Na_3PO_4. *Science Letters*, 10(2), 26-30. https://scilett-fsg.uitm.edu.my/

[15] Vijaya, N., Selvasekarananandian, S., Hirankumar, G. & Karthikeyan, S. (2011). Structural, vibrational, thermal, and conductivity studies on proton-conducting polymer electrolyte based on poly (N-vinylpyrrolidone). *Ionics*, 18, 1-2. https://doi.org/10.1007/s11581-011-0589-4

[16] Slesarenko, N. A., Chernyak, A. V., Khatmullina, K. G., Baymuratova, G. R., Yudina, A. V., Tulibaeva, G. Z., Shestakov, A. F., Volkov, V. I. & Yarmolenko, O. V. (2023). Nanocomposite polymer gel electrolyte based on TiO_2 nanoparticles for lithium batteries. *Membranes*, 13, 776. https://doi.org/10.2290/membranes13090776

[17] Majka, T. M., Agnieszka, L. & Krzysztof, P. (2016). Thermal stability and degradation of polymer nanocomposites. *Polymer Nanocomposites*, 167-190. https://doi.org/10.1007/978-3-319-28238-17

[18] Song, M. Y. & Kwak, Y. J. (2022). Determination of the activation energy for hydride decomposition using a sieverts-type apparatus and the Kissinger equation. *Metals*, 12(2), 265. https://doi.org/10.3390/met12020265

[19] Tsurumaki, A., Rettaroli, R., Mazzapioda, L. & Navaira, M.A. (2022). Inorganic-organic hybrid electrolytes based on AI-doped $Li_7La_3Zr_2O_{12}$ and ionic liquids. *Applied Science*, 12, 7318. https://doi.org/10.3390/app12147318

[20] Wang, H., Xu, Y., Zhang, Y. & Song, Y. (2019). Thermogravimetric analysis and thermal Stabilityof polymer electrolytes for lithium batteries. *Journal of Thermal Analysis and Calorimetry*, 135, 175-185. https://doi.org/10.1007/s10973-018-7029-9

[21] Vyazovkin, S. (2020). Activation energies and temperature dependencies of the rates of crystallization and melting of polymers. *Polymers*, 12(5), 1070. https://doi.org/10.3390/polym12051070

[22] Vyazovkin, S., Burnham, A. K., Criado, J. M., Perez-Maqueda, L. A., Popescu., C. & Sbirrazzuoli, N. (2011). ICTAC kinetics Committee recommendations for performing kinetic computations on thermal analysis data. *Thermochimica Acta*, 520(1-2), 1-19. https://doi.org/10.1016/j.tca.2011.03.034

[23] Wijanarko, N. P., Wulandari, D., Arrafii, M. H., Pradanawati, S. A., Nimah, Y. L., Noerochim, L. & Hamidah, N. L. (2024). Effect of solid polymer electrolyte based on corn starch and lanthanum nitrate on the electrochemical performance of supercapacitor. *Bio Web of Conferences*, p. 03001. https://doi.org/10.1051/biocontf/20248903001

Citing this Article

Iyamu, C. O., Ewa, I. I., & Lumbi, L. W. (2026). Thermal stability analysis of cassava starch-polyvinylpyrrolidone nanocomposite polymer electrolytes using Kissinger model for lithium-ion battery applications. *Lafia Journal of Scientific and Industrial Research, 4*(1), 168–174. https://doi.org/10.62050/ljsir2026.v4n1.776